AIP | Applied Physics Letters

Acceptors in ZnO nanocrystals: A reinterpretation

W. Gehlhoff and A. Hoffmann

Citation: Appl. Phys. Lett. **101**, 262106 (2012); doi: 10.1063/1.4773524
View online: http://dx.doi.org/10.1063/1.4773524
View Table of Contents: http://apl.aip.org/resource/1/APPLAB/v101/i26
Published by the American Institute of Physics.

Related Articles

Two-dimensional electronic spectroscopy of CdSe nanoparticles at very low pulse power
J. Chem. Phys. 138, 014705 (2013)

Tip-enhanced sub-diffraction fluorescence imaging of nitrogen-vacancy centers in nanodiamonds
Appl. Phys. Lett. 102, 013102 (2013)

Investigation of the thermal charge “trapping-detrapping” in silicon nanocrystals: Correlation of the optical properties with complex impedance spectra
Appl. Phys. Lett. 101, 242108 (2012)

Ultrabroadband terahertz conductivity of Si nanocrystal films
Appl. Phys. Lett. 101, 211107 (2012)

Spectral patterns underlying polarization-enhanced diffractive interference are distinguishable by complex trigonometry
Appl. Phys. Lett. 101, 183104 (2012)

Additional information on Appl. Phys. Lett.

Journal Homepage: http://apl.aip.org/
Journal Information: http://apl.aip.org/about/about_the_journal
Top downloads: http://apl.aip.org/features/most_downloaded
Information for Authors: http://apl.aip.org/authors

ADVERTISEMENT

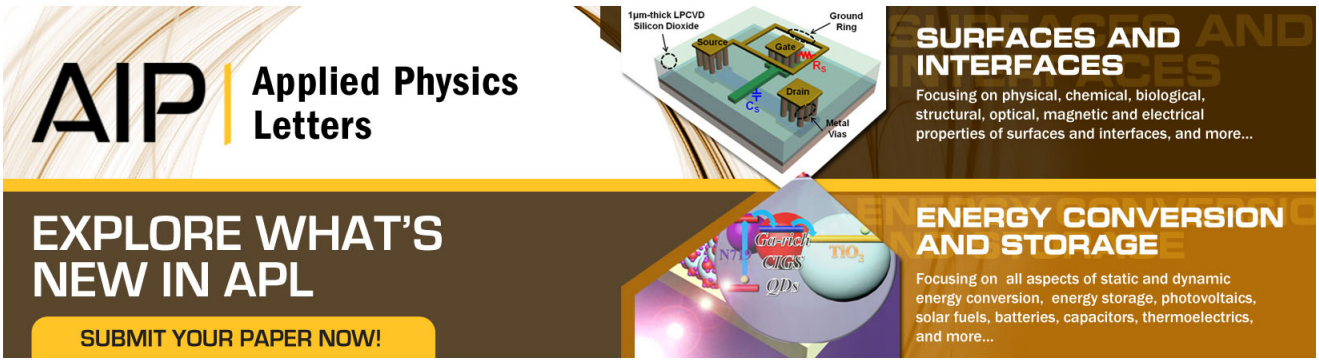

Acceptors in ZnO nanocrystals: A reinterpretation

W. Gehlhoff[a] and A. Hoffmann
Institut für Festkörperphysik, Technische Universität Berlin, Hardenbergstraße 36, 10623 Berlin, Germany

(Received 14 October 2012; accepted 13 December 2012; published online 28 December 2012)

In a recent article, Teklemichael *et al*. reported on the identification of an uncompensated acceptor in ZnO nanocrystals using infrared spectroscopy and electron paramagnetic resonance (EPR) in the dark and under illumination. Most of their conclusions, interpretations, and suggestions turned out to be erroneous. The observed EPR signals were interpreted to originate from axial and nonaxial V_{Zn}-H defects. We show that the given interpretation of the EPR results is based on misinterpretations of EPR spectra arising from defects in nanocrystals. The explanation of the infrared absorption lines is in conflict with recent results of valence band ordering and valence band splitting. © *2012 American Institute of Physics*. [http://dx.doi.org/10.1063/1.4773524]

Bulk material, epitaxial layers, and nanostructures of zinc oxide (ZnO) have attracted great attention over the past decades due to their potential for the realization of optoelectronic, spintronics, and sensor devices.[1–3] Therefore, it is very important to realize the controllable growth of ZnO structures and to investigate their electronic and optical properties, which are extremely sensitive to defects and impurities that have localized electronic states with energy levels in the band gap. Especially, for a resolution of the so-called p-type problem in ZnO (Ref. 4), a deeper insight into the nature of acceptor centers in ZnO and elaboration on techniques for improving p-type impurity incorporation are required.

Recently, Teklemichael, Hlaing Oo, McCluskey *et al*.[5] (THC) reported on the identification of an uncompensated acceptor in ZnO nanocrystals using infrared (IR) spectroscopy and electron paramagnetic resonance (EPR). IR absorption measurements at low temperatures suggest a hydrogenic acceptor with a hole binding energy of 0.4–0.5 eV. By EPR measurements in the dark, they found a resonance at $g = 2.003$, which was attributed to an acceptor involving a zinc vacancy. After illumination of the sample, additional signals at $g = 2.013$ and near $g = 2.003$ occur, which are attributed to nonaxial and axial V_{Zn}-H complexes, respectively. Among other acceptor-like lines, such V_{Zn}-H complexes were recently proved by Kappers *et al*.[6] and Evans *et al*.[7] in electron-irradiated ZnO crystals. Based on these observations, THC[5] speculated on the nature of the hydrogenic acceptor.

We have some serious comments on their analysis of the observed EPR spectra and especially on their conclusions that the EPR spectra observed after illumination originate from axial and nonaxial vacancy-hydrogen (V_{Zn}-H) pairs in the ZnO nanocrystals. EPR studies have been proven to be most useful for the electronic and geometric characterization of defects in semiconductors. In many cases, also the chemical identity of the studied defects can unambiguously be identified through the observation of a characteristic hyperfine interaction. However, the analysis of EPR spectra of nanocrystals requires special carefulness, because a random distribution of the orientation of the axes of the nanocrystals has to be taken into account which hinders a direct comparison and unique assignment to EPR spectra of single crystals. We show by computer simulations that the observed spectra cannot arise from (V_{Zn}-H) pair defects. Therefore, the given discussion of the apparent connection between the hydrogenic acceptor detected by IR measurements and the defects observed by EPR with and without illumination, as well as the nature of the acceptor, is based on erroneous assumptions.

The spectra of the axial and nonaxial singly ionized zinc vacancy (V_{Zn}^-) in ZnO can be described by the spin Hamiltonian (SH)[8]

$$\mathbf{H} = \mu_{\mathbf{B}} \mathbf{S} \mathbf{g} \mathbf{B}, \tag{1}$$

with $S = 1/2$. EPR investigations show that the hole is located on one of the four adjacent single oxygen neighbors O^{2-} which form a nearly regular tetrahedron. This gives rise to two distinct versions of the negatively charged zinc vacancy (V_{Zn}^-), which are easily distinguished by the different angular dependencies of their line positions. The vacancy having the hole localized on the oxygen neighbor located along the c axis is referred to as the axial center, while a vacancy having the hole localized on one of the three basal oxygen neighbors of the (0001) face is referred to as a nonaxial center. These three nonaxial defects have monoclinic C_{1h} symmetry and the g-matrix of each defect is described by three different principal values, whereas the axial defects have C_{3V} symmetry and the g-matrix can be described by the two principal values $g_{\parallel}$ and $g_{\perp}$. Using the magnitudes and principal axes of the g-matrix determined by several authors,[8–11] we have calculated the angular dependencies of the axial and nonaxial defects. We note that the small differences in the published values[8–11] are not relevant for the following considerations. For the spectra presented in Figs. 1 and 2, we used the parameters given by Galland and Herve:[8] (1) $g_{\parallel} = 2.0024$ and $g_{\perp} = 2.0193$ for the axial centers and (2) $g_{xx} = 2.0173$, $g_{yy} = 2.0183$, $g_{zz} = 2.0028$, and $\alpha = 110.75°$ for the non-axial centers. Here, the z- and x-axes are located in a {1120} reflection symmetry plane and α is the angle between the z- and c-axes. The resulting X-band line

[a]Author to whom correspondence should be addressed. Electronic mail: gehlhoff@sol.physik.tu-berlin.de. Tel.: +493031426601. Fax: +4930314 22569.

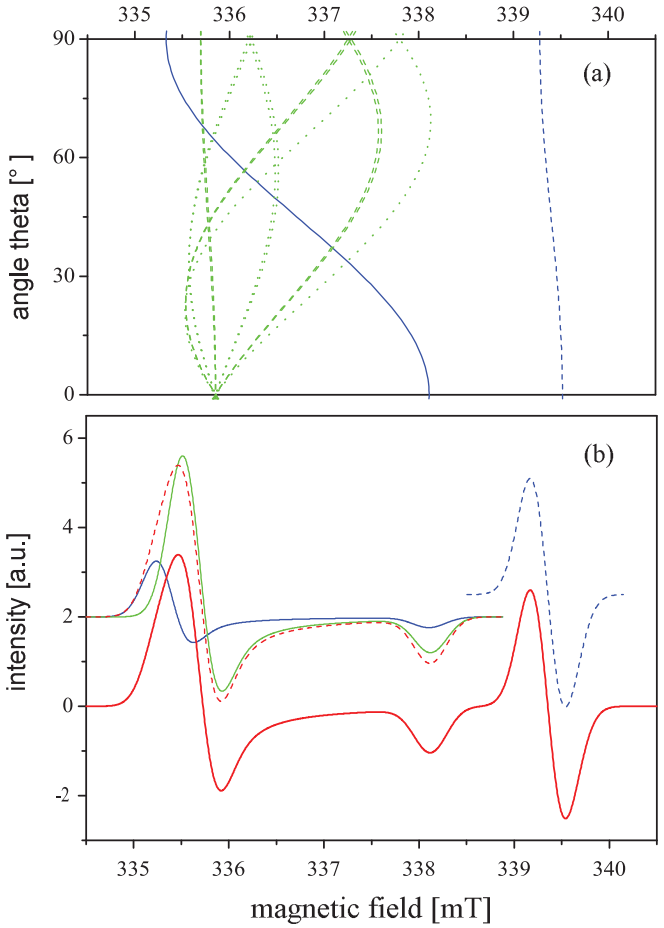

FIG. 1. EPR line positions and powder-spectra of the axial (blue solid line) and nonaxial (green lines) configuration of the negatively charged zinc vacancy (V_{Zn}^{-}) in ZnO at 9.47826 GHz, including the signal from the singly ionized oxygen vacancy (V_0^+) (blue dashed line): (a) The magnetic field is rotated by the angle theta around the $[1\bar{2}10]$- and $[10\bar{1}0]$-axes perpendicular to the c-axis (dashed and dotted lines, respectively). To reveal the six magnetically inequivalent nonaxial sites, a misorientation of the given rotation axis of 0.5° was assumed. (b) Calculation of the powder-like total spectrum (red solid line) consisting of the V_{Zn}^{-} sum spectrum (red dashed line) and V_0^+ spectrum (blue dashed line). (The spectra are shifted vertically for clarity.)

positions are shown for the axial and nonaxial defects in Fig. 1 for rotations around (a) the c-axis and (b) the $[1\bar{2}10]$- and $[10\bar{1}0]$- axes perpendicular to the c-axis. Because there are two cation sites separated by a 180° rotation around c in the unit cell of a hexagonal crystal, there is a total of six magnetically inequivalent sites for these nonaxial defects and therefore six different line positions for arbitrary directions of the magnetic field, which fall partly together for selected rotation planes.

For the calculation of the zinc vacancy spectra in ZnO powder, a random distribution of the orientation of the axes of the nanocrystals has to be taken into account. This was done by integration of the EPR lines for the different center orientations over the full space angle. Using the EasySpin software package,[12] we solved the SH (1) by exact diagonalization for the axial and nonaxial centers for the two cation sites in the wurtzite structure. The EPR spectra for the axial and nonaxial defects as well as the sum spectrum resulting from the weighted sum of both spectra are shown in Fig. 1(b), exhibiting the typical lineshape for defects with anisotropic g-values in powder-like materials. For the calculation

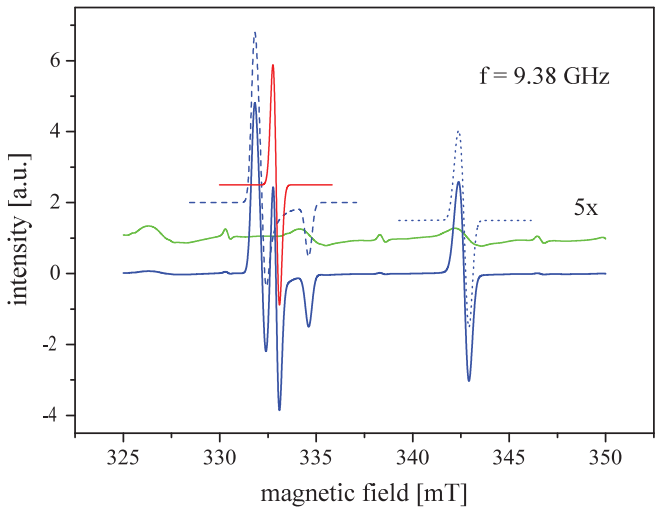

FIG. 2. Simulated total EPR powder-spectrum (blue solid line) of defects in ZnO at 9.38 GHz including the axial and nonaxial configuration of the negatively charged zinc vacancy (V_{Zn}^{-}) (blue dashed line), the shallow donor signal (blue dotted line), and a small contribution of residual Mn^{2+} (green solid line) as well as a nearly isotropic line with g = 2.013 (red solid line). (The spectra are shifted vertically for clarity.)

of the presented sum spectra, we assume that the ratio of the axial to nonaxial paramagnetic defects is given by the ratio 1:3 (2:6) of the corresponding lattice sites. This assumption requires that the capture of a hole at the four surrounding oxygen ions occurs with equal probability. In reality, trapping of the hole on basal oxygen is energetically favored as compared to the axial configuration with the defect axis z along the c-axis of the crystal. Additionally, one has to consider that due to the illumination of the samples, there is a competition between the trapping of the holes and the temperature dependent depopulation of the axial defects. Therefore, the resulting relative intensity between both spectra is determined by the achieved steady-state population of the two types of defects, which depends on the temperature and on the intensity of the illumination.

However, deviations of the used 1:3 ratio cause only changes of the lineshape and lineposition of the low-field line (see Fig. 1(b)) which hardly affect the following considerations. To simplify a direct comparison with the published results,[6,7] the presented total spectrum includes in addition the contribution[13] of the singly ionized oxygen vacancy (V_0^+). However, THC[5] assigned the EPR spectra of the investigated nanocrystals not to isolated zinc vacancies but to ones having an OH^- ion at an adjacent oxygen site. As mentioned above, such defects were recently detected by Kappers *et al.*[6] and Evans *et al.*[7] in electron-irradiated ZnO bulk crystals. They found two doublets labeled as centers D and E in (Ref. 7) very close to the isolated axial and nonaxial singly ionized zinc vacancy, respectively. According to the given interpretation, the center D has the unpaired spin localized on the axial neighbor with the OH^- ion at one of the three neighboring nonaxial oxygen sites, while the center E has the unpaired spin localized on one of the three nonaxial neighbors with the OH^- ion at one of the other two nonaxial oxygen sites or at the axial oxygen site. Unfortunately, neither the principal g-values of the centers D and E nor spectra for other magnetic field directions except B||c were given in

both papers. However, from the small changes of the line positions shown in Fig. 1 (Ref. 7) and Fig. 5 (Ref. 6) for B||c and the observed small changes of the g-values[10] for the non-axial zinc vacancy adjacent to interstitial Zn_i^0 ($V_{Zn}^- : Zn_i^0$), we can assume that the additional association of hydrogen to the defects will hardly change the principal values. Therefore, a quite similar spectrum as shown in Fig. 1 with marginally shifted line positions will be obtained for these (V_{Zn}-H) defects in nanocrystals. To simplify the comparison with Fig. 3 in Ref. 5, we present in Fig. 2 the corresponding spectrum for a microwave frequency f = 9.38 GHz and a larger magnetic field region as used in Ref. 5. In addition, we include contributions of the shallow donor resonance[13] with g ≃ 1.956 and small lines due to residual Mn^{2+} (S = 5/2, I = 5/2) impurities in the core of the nanocrystals[14] to the total spectrum.

Comparing Fig. 2 with Fig. 1 in Ref. 5, it is evident from the differences in the line positions and the line shapes that the observed lines in Ref. 5 can never be attributed to the axial and nonaxial V_{Zn}-H defects. As corresponding simulations with the parameter given in Ref. 10 reveal, also the bi-vacancy $(V_{Zn}^-)_2^-$ can be excluded. The line shapes for the resonances at g = 2.003 and g = 2.013 indicate that both resonances are caused by defects with isotropic or at least nearly isotropic g-values. The line with g = 2.013, which is observed only after illumination with a xenon lamp and which is misleadingly assigned to nonaxial, paramagnetic $V_{Zn}^- - H^+$ defects,[5] is probably caused by a photosensitive impurity. From the g-value and the behavior under light at T = 77 K, it is consistent with the main signal originates by Pb^{3+},[15] which is a common impurity in ZnO powder.

Direct evidence of Pb^{3+} impurities can be obtained by more sophisticated EPR measurements, because the main signal at g = 2.013 caused by the zero-spin Pb-isotopes ^{204,206,208}Pb is accompanied by two weaker signals[15] originate from the isotope ^{207}Pb with I = 1/2 and the natural abundance of 21.1%. For a microwave frequency of 9.38 GHz, these transitions are placed at 5205 G and 18206 G, originating from the ($F = 1, m_F = -1$) ↔ ($F = 1, m_F = 0$) and ($F = 1, m_F = 0$) ↔ ($F = 1, m_F = +1$) transitions, respectively.[16] The line with the isotropic spin-only g-value g = 2.003 suggests as origin a residual impurity with an S ground state and without or small hyperfine splitting, too. However, missing data about the conditions of the EPR measurements prevent us from making more complete consideration. It should be noted here that for a reliable interpretation, more detailed EPR investigations connected with measurements at low temperatures are necessary. Furthermore, the authors should provide evidence that this line is related neither to the basic cavity line nor to light-induced centers caused in the quartz Dewar and tubes used for the EPR measurements by the illumination of the samples with the xenon lamp.

From the discussion given above, it is clear that the observed lines cannot be assigned to V_{Zn}-H defects as stated by THC.[5] In addition, we remark that also the claimed production of new defects at g = 2.003 under illumination follows not stringently from the presented data. Figs. 3(a) and 3(b) in Ref. 5 show that not only the intensity of the line at g = 2.003 but also the intensity of the shallow donor line increases under illumination approximately by the same factor. For a sound analysis of this behavior, it is required that light-induced changes of the sample conductivity and a possible partial desaturation of both signals can be ruled out or taken into account by calibration of the spectrometer sensitivity and power-dependent measurements of the signal intensities, respectively. There again, the observed light-induced increase of the intensity of both lines can also be connected with the same recharging ratio of both defects and must not be solely connected with the production of other ones.

Concerning the interpretation of the observed five strongest IR absorption peaks, we restrict ourselves to a few remarks. The observed five main absorption peaks were assigned without detailed analysis to the transitions to the excited states of a hydrogenic acceptor with holes originating from the A and B valence bands and assuming the valence band ordering given by Reynolds *et al.*[17] with the topmost A valence band with Γ_9 symmetry. The measured offset of 15 meV between the two line sets is identified as the energy separation between the A and B excitons reported to be 15 meV at low temperature.[18] However, recent magneto-optical studies confirmed the originally proposed valence band ordering by Thomas and Hopfield[19] that the uppermost A valence band possesses Γ_7 symmetry[20] in contrast to most II-VI wurtzite structures. In addition, the valence band splitting Δ_{AB} is around 4.5 meV.[21,22] There are some doubts that the stress existing in nanocrystals with an average diameter of 20 nm can reverse the valence band ordering and change the value of Δ_{AB} to 15 meV.

In summary, we have demonstrated by numerical calculations and advanced considerations that the observed EPR spectra in ZnO nanocrystals presented by THC[5] cannot be attributed to the axial and nonaxial zinc vacancy associate with hydrogen (V_{Zn}-H). The observed spectra are probably caused by unknown impurities with nearly isotropic g-values. Also, the implied connection of the observed EPR lines with the assumed hydrogenic acceptor found by IR absorption measurements is untenable. In addition, the explanation of the IR absorption lines is in conflict with recent results of valence band ordering and valence band splitting.

[1]Z. L. Wang, J. Phys.: Condens. Matter **16**, R829 (2004).
[2]A. Janotti and C. G. Van de Walle, Rep. Prog. Phys. **72**, 126501 (2009).
[3]Ü. Özgür, D. Hofstetter, and H. Morkoc, Proc. IEEE **98**, 1255 (2010).
[4]V. Avrutin, D. J. Silversmith, and H. Morkoc, Proc. IEEE **98**, 1269 (2010).
[5]S. T. Teklemichael, W. M. Hlaing Oo, M. D. McCluskey, E. D. Walter, and D. W. Hoyt, Appl. Phys. Lett. **98**, 232112 (2011).
[6]L. A. Kappers, O. R. Gilliam, S. M. Evans, L. E. Halliburton, and N. C. Giles, Nucl. Instrum. Methods Phys. Res. B **226**, 2953 (2008).
[7]S. M. Evans, N. C. Giles, L. E. Halliburton, and L. A. Kappers, J. Appl. Phys. **103**, 043710 (2008).
[8]D. Galland and A. Herve, Phys. Lett. **33A**, 1 (1970); Solid State Commun. **14**, 953 (1974).
[9]A. L. Taylor, G. Filipovich, and G. K. Lindberg, Solid State Commun. **8**, 1359 (1970).
[10]B. Schallenberger and A. Hausmann, Z. Phys. B **23**, 177 (1976).
[11]L. S. Vlasenko and G. D. Watkins, Phys. Rev. B **72**, 035203 (2005).
[12]S. Stoll and A. Schweiger, J. Magn. Reson. **178**, 42 (2006).
[13]L. S. Vlasenko, Appl. Magn. Reson. **39**, 103 (2010).
[14]A. O. Ankiewicz, W. Gehlhoff, J. S. Martins, A. S. Pereira, S. Pereira, A. Hoffmann, E. M. Kaidashev, A. Rahm, M. Lorenz, M. Grundmann, M. C. Carmo, T. Trinade, and N. Sobolev, Phys. Status Solidi B **246**, 766 (2009).
[15]G. Born, A. Hofstaetter, and A. Scharmann, Phys. Lett. **36A**, 447 (1971).

[16]Because the large hyperfine interaction of the $^{207}Pb^{3+}$ ion ($A = 0.8080\,cm^{-1}$) dominates the Zeeman term in the X-band ($\approx 0.3\ cm^{-1}$), the spin vectors **S** and **I** are coupled together at these low magnetic fields to the total vector F, and the corresponding eigenvalues and EPR transitions are given by the Breit-Rabi formula.
[17]D. C. Reynolds, C. W. Litton, and T. C. Collins, Phys. Rev. **140**, A1726 (1965); D. C. Reynolds, D. C. Look, B. Jogai, C. W. Litton, G. Cantwell, and W. C. Harsch, Phys. Rev. B **60**, 2340 (1999).
[18]C. Boemare, T. Monteiro, M. J. Soares, J. G. Guilherme, and E. Alves, Physica B **308–310**, 985 (2001).
[19]D. G. Thomas, Phys. Chem. Solids **15**, 86 (1960); J. J. Hopfield, *ibid.* **15**, 97 (1960).
[20]M. R. Wagner, J.-H. Schulze, R. Kirste, M. Cobet, A. Hoffmann, C. Rauch, A. V. Rodina, B. K. Meyer, V. Röder, and K. Thonke, Phys. Rev. B **80**, 205203 (2009).
[21]B. K. Meyer, J. Sann, S. Lautenschläger, M. R. Wagner, and A. Hoffmann, Phys. Rev. B **76**, 184120 (2007).
[22]B. K. Meyer, J. Sann, S. Eisermann, S. Lautenschläger, M. R. Wagner, M. Kaiser, G. Callsen, J. S. Reparaz, and A. Hoffmann, Phys. Rev. B **82**, 115207 (2010).